Supplemental Material and Methods

Construction of Rng2p and Rng2p deletion mutants

The integration cassette for mEGFP-Rng2p was constructed by cloning *rng2*, along with its promoter and an N-terminal mEGFP into pJK148 using the BamHI and SalI restriction sites. To construct each Rng2p deletion vector, the pJK148 Prng2-mEGFP-Rng2p plasmid was amplified using primers homologous to the regions flanking the area to be deleted. Each primer contained an NsiI cut site, and the PCR product was cut with NsiI and then re-ligated using a Rapid Ligation kit (Roche). The resulting plasmids were transformed into Top10 cells and amplified before isolation using Qiagen Miniprep kit (Qiagen). Each plasmid was sequenced to confirm the deletion of the desired domain and integrity of the remaining sequence. The deletions were designed to encode five glycine residues in addition to the two residues encoded by the NsiI cut site. This created a flexible linker between domains rather than potentially forcing the remaining domains into a constrained conformation. This linker does not replace the 4 glycine linker between the N-terminal GFP and the beginning of the Rng2p construct, except in the case of Rng2ΔCHD where the deletion (and the longer linker) immediately follows the GFP. After sequencing, each plasmid was linearized with NruI and purified with a Qiagen PCR purification kit (Qiagen). The resulting linear DNA was integrated into *S. pombe* cells by the lithium acetate integration method. Untagged Rng2p and Rng2p deletion constructs were made using the same protocol, but beginning with pJK148 with only *rng2* and its promoter cloned into the BamHI and SalI sites.

Expression and Purification of the Rng2pCHD

Rng2pCHD was purified similar to a published purification method (Wang et al, 2003). The sequence of the CHD was amplified from genomic DNA using primers with BamHI and SalI restriction sites, cloned into the pGEX6P vector and sequenced. The pGEX6P-Rng2pCHD plasmid was transformed into BL21(RIL) (Stratagene) cells for expression. Cells were grown to an OD_{600} = 0.6 at 37°C, then induced with 0.5 mM IPTG and grown for 16 h at 16°C. Cells were pelleted at 6000 r.p.m. for 10 min in a Beckman JLA-10.5 rotor at 4°C, re-suspended in lysis buffer (50 mM Tris pH 8, 300 mM NaCl, 2 mM DTT) and broken by sonication. The cell debris was pelleted by centrifugation at 16,000 r.p.m. for 30 min in a Beckman JA 30.5 rotor at 4°C. The soluble protein was bound to washed glutathione-Sepharose beads for 1 h at 4°C. The beads

and protein were loaded into a column and unbound proteins eluted with 3 column volumes of lysis buffer, before GST-Rng2pCHD was eluted with elution buffer (50 mM glutathione, 50 mM Tris pH 8, 150 mM NaCl, 2 mM DTT). GST-Rng2pCHD was reacted overnight with PreScission Protease (GE) according to the manufacturer's instructions. The cleaved GST and uncleaved proteins were rebound to fresh glutathione-Sepharose beads and the cleaved Rng2pCHD was eluted with PreScission cleavage buffer (50 mM Tris-HCl, 150 mM NaCl, 1mM EDTA, 1mM DTT pH 7). Rng2pCHD was purified on a 2 x 60 cm Sephacryl S200 gel filtration column equilibrated in cleavage buffer to remove residual GST and uncleaved protein.

Actin filament binding experiments

Chicken skeletal muscle actin was purified as previously described (MacLean-Fletcher & Pollard, 1980) with a final purification step of gel filtration in buffer G (2 mM Tris, pH 8.0, 0.2 mM ATP, 0.5 mM DTT, 0.1 mM $CaCl_2$, 1 mM NaN_3). Monomeric Ca^{2+}-ATP-actin in G-buffer (2 mm Tris-HCl pH 8.0, 0.1 mm $CaCl_2$, 1 mm NaN_3, 1 mm DTT) was converted to Mg^{2+}-ATP-actin by the addition of concentrated solution to give 0.05 mM $MgCl_2$, 0.2 mM EGTA. Mg^{2+}-ATP-actin was polymerized by the addition of concentrated KMEI buffer to give final concentrations of 50 mM KCl, 1 mM $MgCl_2$, 1 mM EGTA, 10 mM imidazole, pH 7, for 30 min at 25 °C and then centrifuged at 63,000 r.p.m. for 30 min to pellet the actin filaments. The pellets were resuspended in a minimum volume of 30 µL buffer using a water bath sonicator for 1 min. Rng2pCHD was added to the concentrated actin filaments and incubated for 2 h at 25°C to allow for binding and polymerization of the actin filaments. Actin filaments were separated from the supernatant by spinning the samples at 63,000 r.p.m. for 30 min in a Beckman TLA-100 rotor at 4°C. The proteins in the supernatants were analyzed by SDS-PAGE and visualized by Coomassie Blue staining.

Purification of recombinant proteins for binding experiments

Purification of the first three domains of anillin Mid1p (Mid1 M1-13) was previously described (Saha & Pollard, 2012). Rng2p C-half was cloned into a pMalC2E vector with a sequence encoding 6xHis on the N-terminus of MBP. Rng2p (amino acids 805-1489) was inserted into the modified vector using the BamHI and SalI cut sites and transformed into BL21(RIL) cells. Expression of the fusion protein was induced with 0.5 mM IPTG for 16 hours at 16°C. Cells

were re-suspended in lysis buffer (20 mM Tris pH 8, 300 mM NaCl, 1 mM TCEP and 10 mM imidazole, final pH adjusted to 8.0 at 4°C) and then lysed by sonication. Occasionally, lysozyme was added to aid with lysis. The cell debris was pelleted by centrifugation at 16,000 r.p.m. for 30 min in a JA 30.5 rotor at 4°C. The soluble protein was bound to 2 ml of washed Ni-NTA beads per liter of cell culture for 1 h at 4°C. The beads and protein were loaded into a column and unbound proteins eluted with 3 column volumes of wash buffer (20 mM Tris pH 8, 300 mM NaCl, 1 mM TCEP and 25 mM imidazole), before His-MBP-Rng2pC-half was eluted with elution buffer (20 mM Tris pH 8, 300 mM NaCl, 1 mM TCEP and 250 mM imidazole). His-MBP-Rng2pC-half was dialyzed into storage buffer (20 mM Tris pH 7.4, 300 mM NaCl, 1 mM TCEP) and then was further purified by passage over a 2x60 cm Sephacryl S200 gel filtration column equilibrated with storage buffer.

Pull down experiments from *S. pombe* cell lysates

For all experiments, equal concentrations of cells were pelleted and re-suspended in the appropriate lysis buffer. Cells expressing mEGFP-Rng2p were re-suspended in 0.25% Triton X-100, 100 mM NaCl, 20 mM phosphate buffer (pH 7.4), 0.2 mM DTT, 1 mM PMSF, 0.1mM Na vanadate, 60 mM β-glycerophosphate with EDTA-free protease inhibitor tablets. Cells expressing mEGFP-Cdc15p or Mid1p-YFP were re-suspended in the same buffer containing 1% TritionX-100. Re-suspended cells were lysed by 6 cycles of 45 sec in the bead beater. Unbroken cells were pelleted at 13,000 r.p.m. for 30 s, and cell debris was removed by pelleting 13,000 r.p.m. in a Beckman Coulter Microfuge 18 for 15 min at 4°C. Ni-NTA beads were bound to the recombinant protein for 30 min at 4°C, then pelleted for 30 s at 500 r.p.m. in an Eppendorf Centrifuge 5415 D and washed into the lysis buffer used for each experiment.

Ni-NTA beads with bound recombinant protein were added to cell lysate and incubated for 90 min at 4°C while rotating. After incubation, beads were pelleted for 30 s at 500 r.p.m. in an Eppendorf Centrifuge 5415 D and a sample of the supernatant was removed for western blot analysis. The pelleted beads were washed 4x with lysis buffer before resuspension in 100 uL of 1x SDS sample buffer at 100°C. Each sample was analyzed by SDS-PAGE and western blotting with an antibody to GFP as described in the main text.

Supplemental Figures

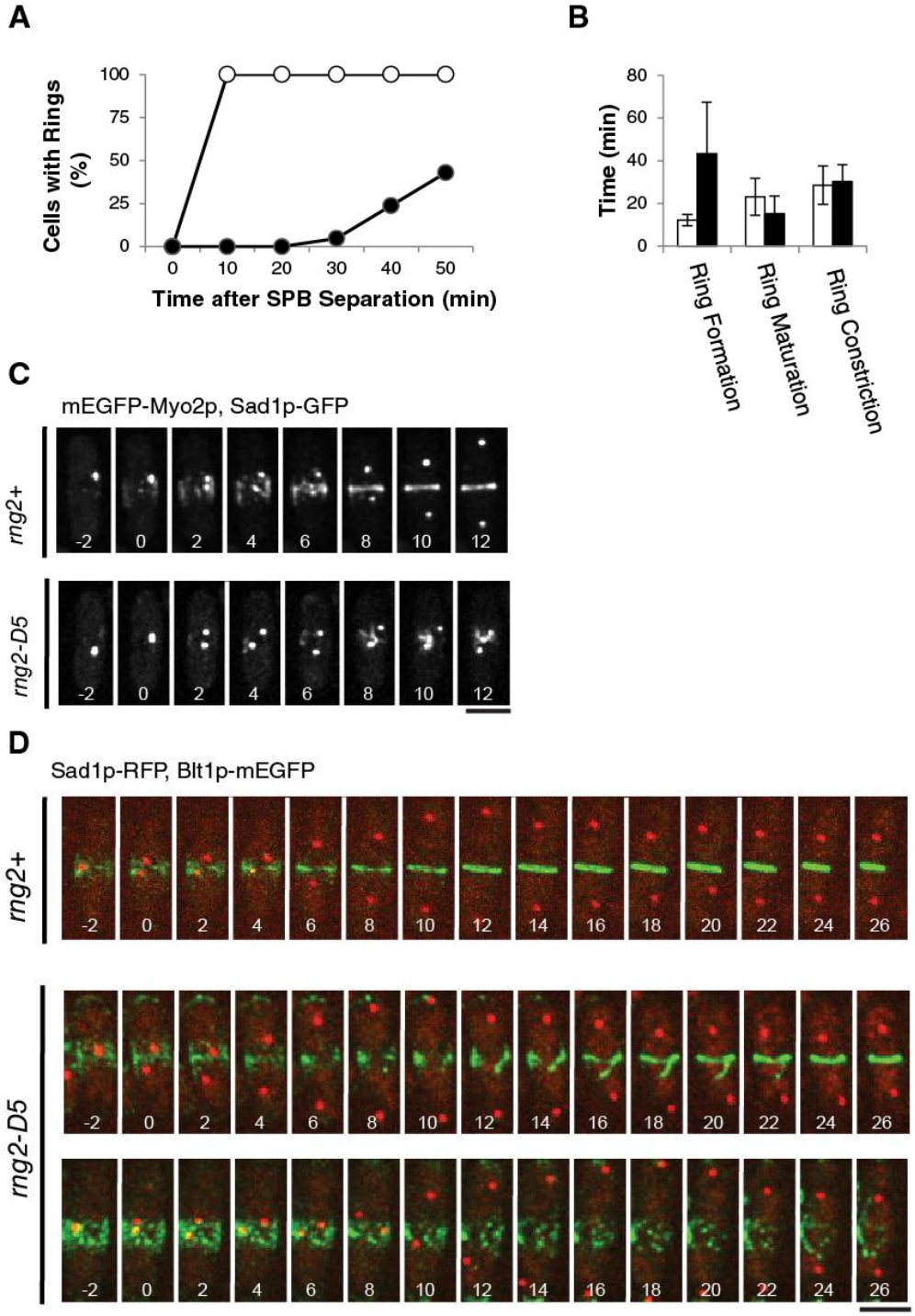

Figure S1. Quantitation of *rng2-D5* phenotypes and node protein localization in *rng2-D5* cells at 32°C. (A) Outcomes graph showing of percent of cells with complete rings of YFP-Cdc15p as a function of time after SPB separation at 32°C: (○) *rng2*$^{+}$ cells; (●) *rng2-D5* cells. (B) Mean

times required (± 1 standard deviation) for WT (open bars) and *rng2-D5* (black bars) cells to assemble (n = 21 and 14, respectively), mature (n = 21 and 19, respectively) and constrict (n = 21 and 24, respectively) contractile rings at 25°C using YFP-Cdc15p as the marker for contractile rings. (C) Time series of fluorescent micrographs recorded at 2 minute intervals at 32°C of *rng2*$^{+}$ (top row) and *rng2-D5* (lower row) cells expressing mEGFP-Myo2p and Sad1-GFP to mark SPBs (both shown in white). Time in min is shown in white with SPB separation defined as time zero. (D) Time series of fluorescent micrographs recorded at 2 minute intervals at 32°C of *rng2*$^{+}$ (top row) and *rng2-D5* (lower row) cells expressing Sad1-RFP to mark SPBs (shown in red) and mEGFP-Blt1p nodes and contractile rings (shown in green). Time in min is shown in white with SPB separation defined as time zero. Each scale bar = 5 μm.

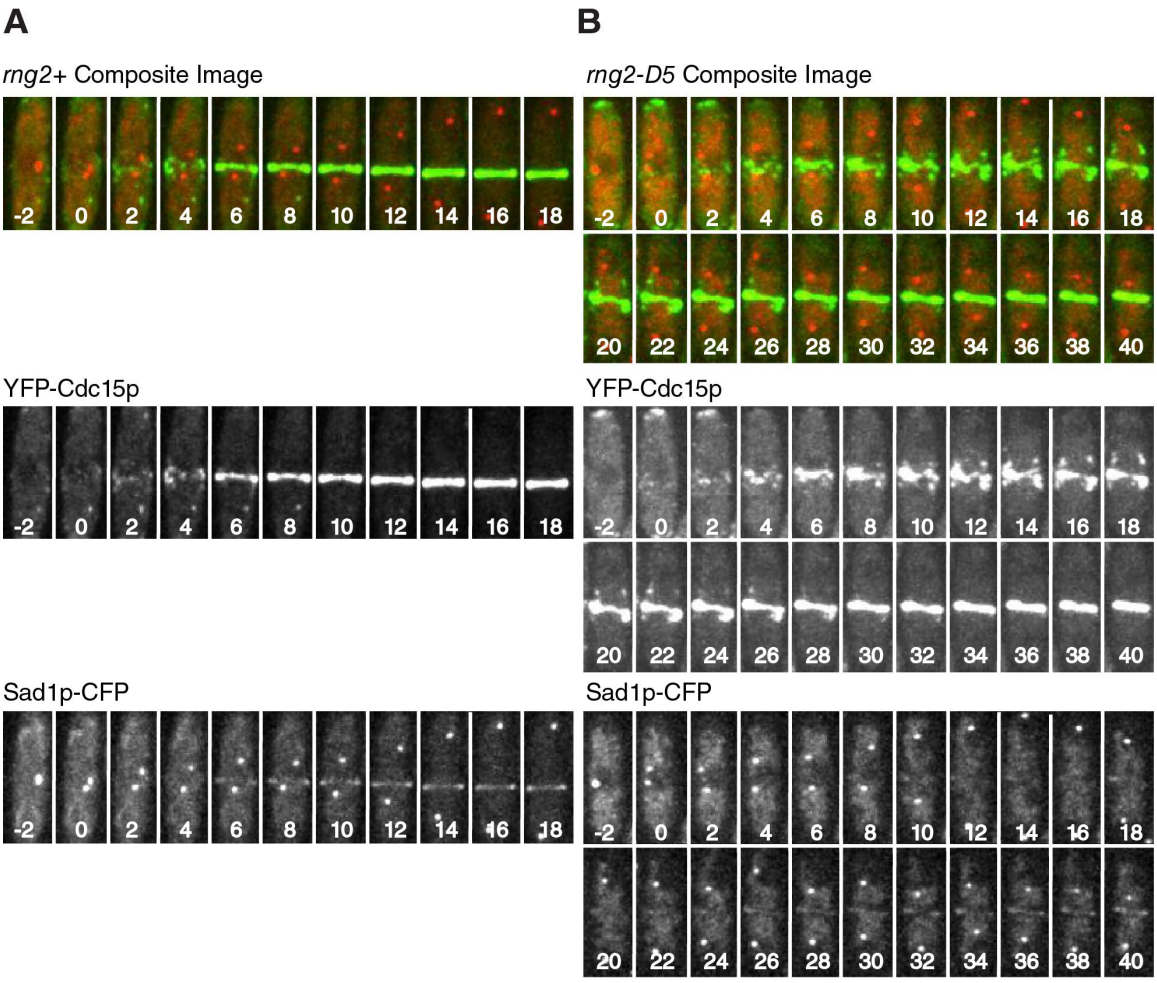

Figure S2. Composite and single channel images of time series of fluorescent micrographs recorded at 2 min intervals of (A) *rng2*$^{+}$ and (B) *rng2-D5* cells expressing Sad1p-CFP and YFP-Cdc15p at 32°C. Time in min is shown in white with SPB separation defined as time zero. Top panels are a composite images showing both Sad1p-CFP (red) and YFP-Cdc15p (green). The middle panels show series of grey scale images of the YFP-Cdc15p signal. The lower panels show series of grey scale images of the Sad1p-CFP signal.

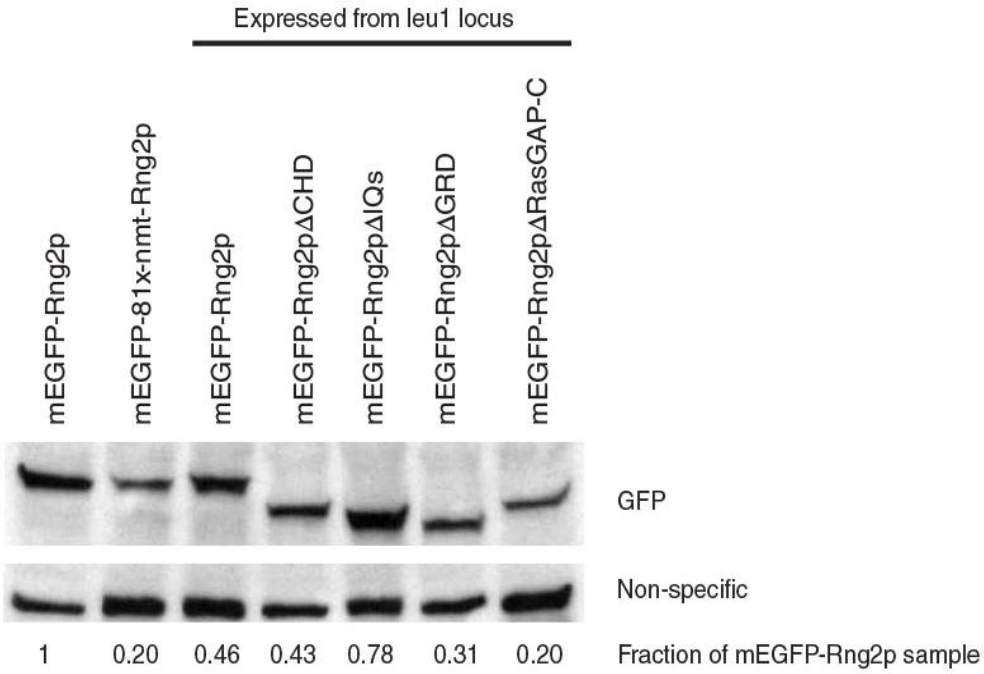

Figure S3. Quantitation of Rng2p expression in wild type and repressed cells.
Otherwise wild type *S. pombe* cells were used to express mEGFP-Rng2p from the native promoter under the control of either the native *rng2* promoter or the *81x-nmt* promoter in repressing conditions. *S. pombe rng2*Δ strains were used to express the following constructs from the *leu1* locus: mEGFP-Rng2p, mEGFP-Rng2pΔCHD, mEGFP-Rng2pΔIQ and mEGFP-Rng2pΔGRD. A *rng2-D5* strain was used to express mEGFP-Rng2pΔRasGAP-C from the *leu1* locus. A sample of each strain was lysed and analyzed for expression by SDS-PAGE and western blotting with an antibody to GFP as described in the main text. The resulting western blot was scanned with a Microtek ScanMaker 6800 and converted to a jpeg file. The density of each GFP-Rng2p band was normalized for loading by comparison with a non-specific band also detected by the anti-GFP antibody. This band is also present in blots of cell extracts that do not contain GFP. The average fraction of Rng2p calculated from three separate experiments is indicated below each lane.

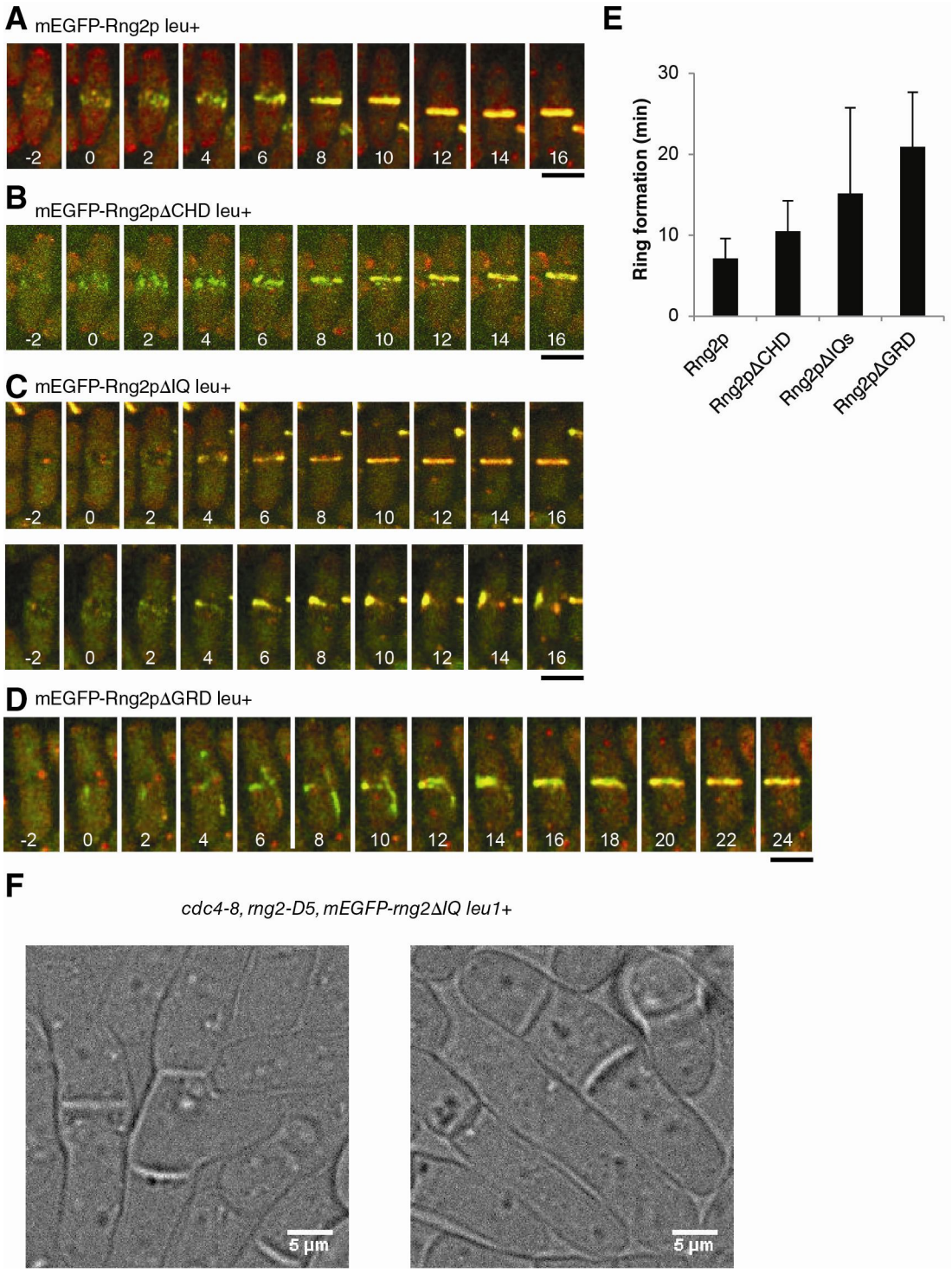

Figure S4. Rng2p constructs lacking each of the first three domains restore the ability of *rng2-D5* cells to form contractile rings. (A-D) Time series of fluorescent micrographs recorded at 2 min intervals at 32°C of *rng2-D5* cells expressing Sad1-RFP (red), mCherry-Cdc15 (red) and the indicated mEGFP-Rng2p construct (green). Time in min is shown in white with SPB separation

defined as time zero. (A) Cells expressing mEGFP-Rng2p. (B) Cells expressing mEGFP-Rng2pΔCHD. (C) Two examples of the phenotypes observed in cells expressing mEGFP-Rng2pΔIQ.The top panel shows a cell that made a contractile ring by condensation of notes. The lower panel shows a cell that made a contractile ring from strands. (D) Cells expressing mEGFP-Rng2pΔGRD. (E) Average time (± 1 standard deviation) required for each strain to form a complete ring following SPB separation (n = 23, 16, 17 and 13 respectively). (F) DIC images of *rng2-D5, mEGFP-Rng2ΔIQ, cdc4-8* cells after 4 h at 36°C. Each scale bar = 5μm.

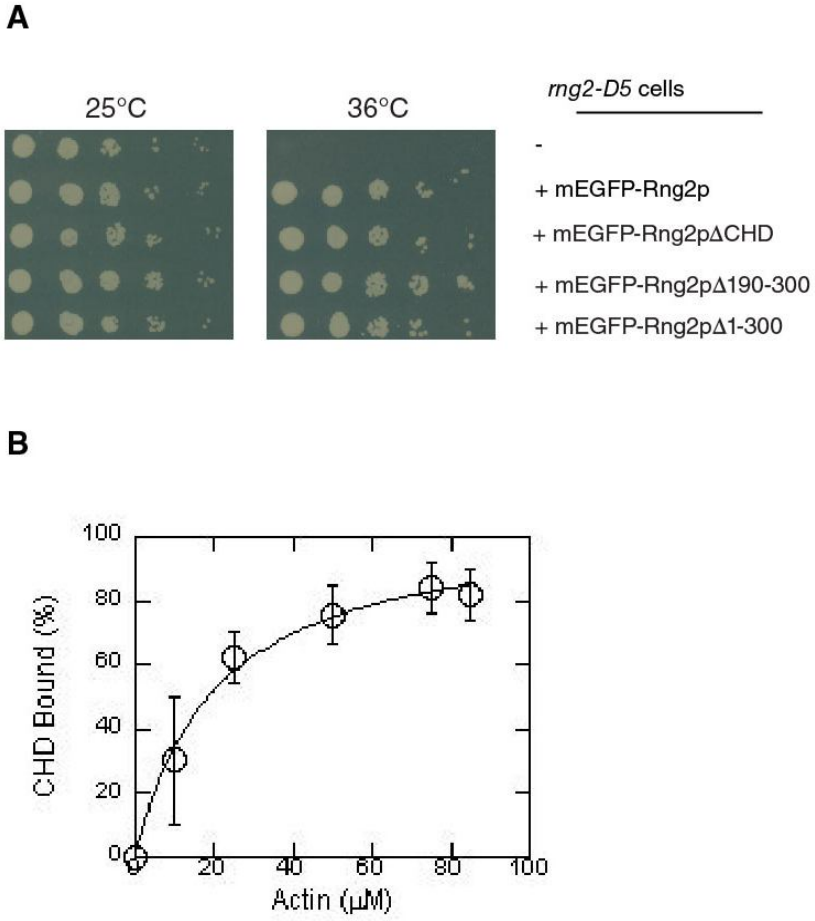

Figure S5. Rng2p constructs lacking the first 300 amino acids of Rng2p rescue the viability of *rng2-D5* cells at the restrictive temperature and Rng2p CHD binds filamentous actin with low affinity. (A) Complementation of *rng2-D5* cells with mEGFP-Rng2pΔCHD, mEGFP-Rng2pΔ190-300, or mEGFP-Rng2pΔ1-300. Photographs of agar plates with spots containing serial 1:10 dilutions of cells incubated 48 h at permissive (25°C) or restrictive (36°C) temperatures. (B) Equilibrium binding of purified Rng2p CHD to actin filaments. Rng2p CHD (1.5 μM) was incubated with a range of concentrations of actin filaments in KMEI buffer at 4°C for 2 h before pelleting at 63,000 r.p.m. for 30 min. Rng2p CHD in the supernatants was measured by gel electrophoresis, staining with Coomassie blue and densitometry, and the bound fraction was calculated by difference from the sample without actin filaments.

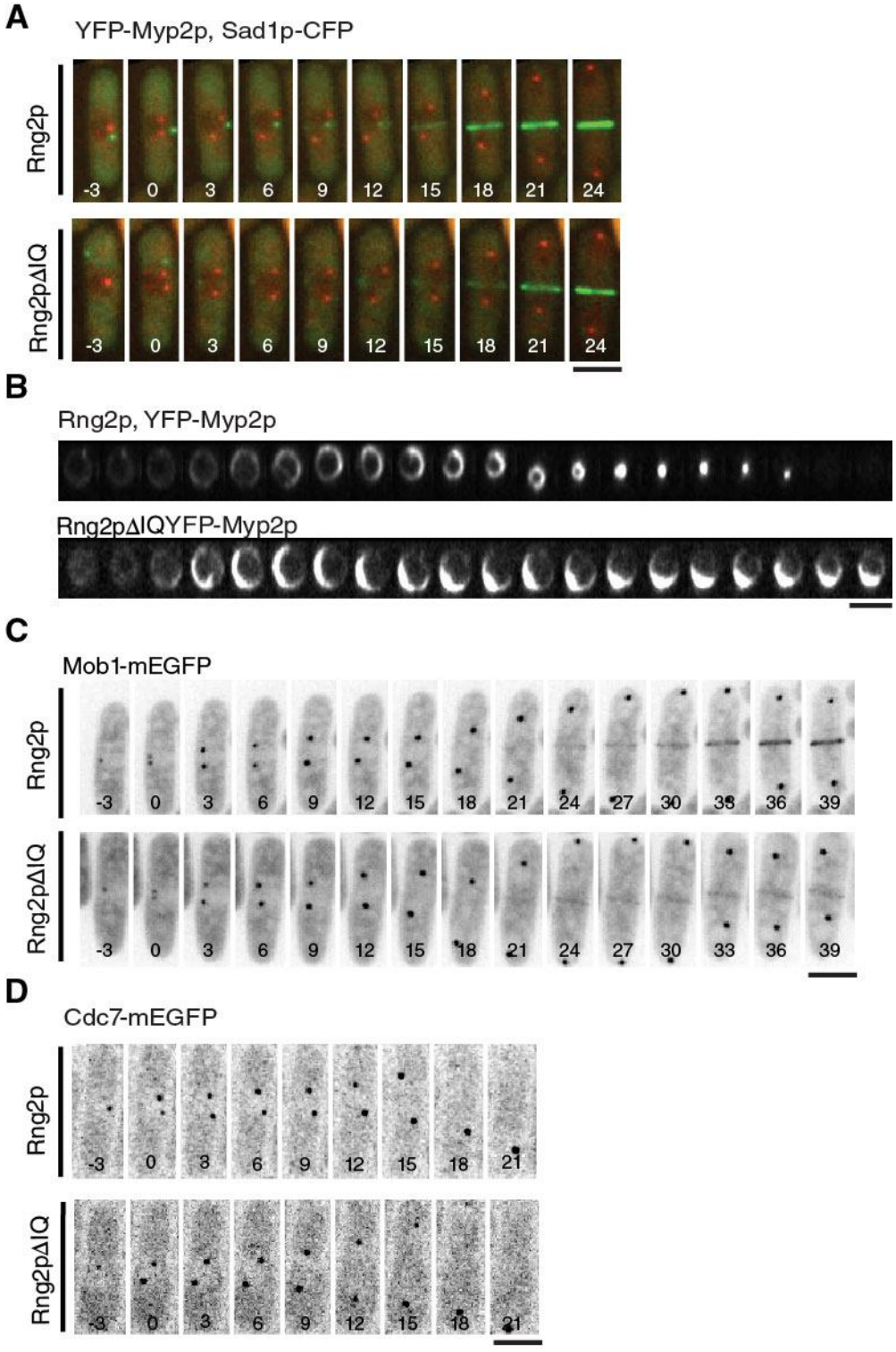

Figure S6. Localization of Mob1p-mEGFP, YFP-Myp2p and Cdc7p-mEGFP in cells dependent on Rng2pΔIQ. (A) Time series of fluorescent micrographs recorded at 3 min intervals at 25°C of

*rng2***Δ** cells complemented with Rng2p (top row) or Rng2pΔIQ (bottom row) expressing YFP-Myp2p (green), and Sad1p-CFP (red). A maximum intensity projection was formed from 20 Z slices collected for each time point. Time in min is shown in white with SPB separation defined as time zero. (B) Time series of 3 dimensional reconstructions of fluorescence micrographs recorded at 3 min intervals at 25°C of *rng2***Δ** cells complemented with Rng2p (top row) or Rng2pΔIQ (bottom row) expressing YFP-Myp2p. The images are Z-sections in the plane of the contractile ring. (C) Time series of negative contrast fluorescent micrographs recorded at 3 min intervals at 25°C of *rng2***Δ** cells complemented with Rng2p (top row) or Rng2pΔIQ (bottom row) expressing Mob1p-mEGFP. A maximum intensity projection was formed from 20 Z slices collected for each time point. Time in min is shown in black with SPB separation defined as time zero. (D) Time series of negative contrast fluorescent micrographs recorded at 3 min intervals at 25°C of *rng2***Δ** cells complemented with Rng2p (top row) or Rng2pΔIQ (bottom row) expressing Cdc7p-mEGFP. Time in min is shown in black with SPB separation defined as time zero. A maximum intensity projection was formed from 20 Z slices collected for each time point. Each scale bar = 5μm.

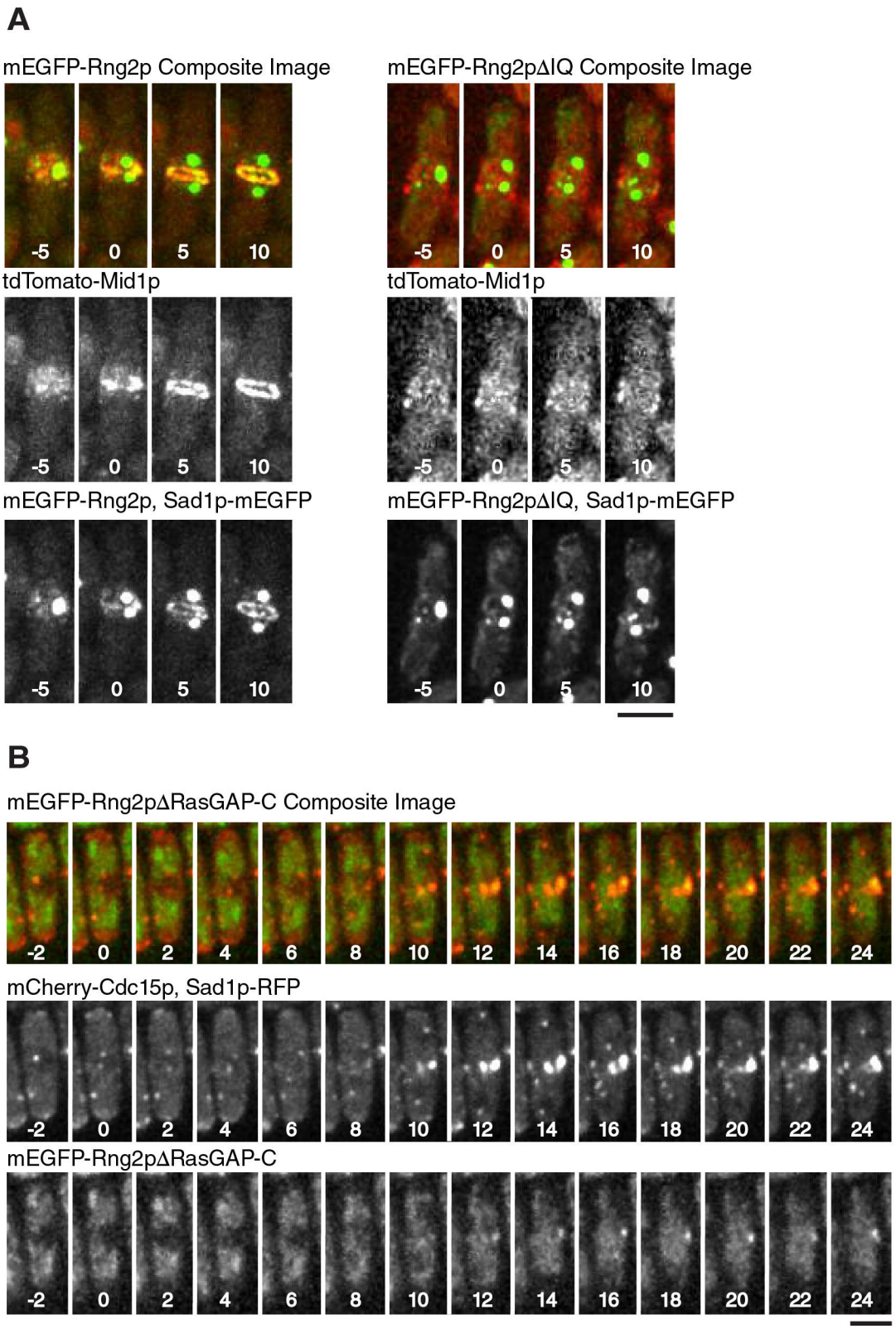
A
mEGFP-Rng2p Composite Image
mEGFP-Rng2pΔIQ Composite Image
-5
0
5
10
tdTomato-Mid1p
tdTomato-Mid1p
mEGFP-Rng2p, Sad1p-mEGFP
mEGFP-Rng2pΔIQ, Sad1p-mEGFP
B
mEGFP-Rng2pΔRasGAP-C Composite Image
-2
0
2
4
6
8
10
12
14
16
18
20
22
24
mCherry-Cdc15p, Sad1p-RFP
mEGFP-Rng2pΔRasGAP-C

Figure S7. Single channel images of mEGFP-Rng2p, mEGFP-Rng2pΔGRD and mEGFP-Rng2pΔRasGAP-C cells. (A) Times series of fluorescent micrographs recorded at 5 min intervals of mEGFP-Rng2p or mEGFP-Rng2pΔGRD cells expressing Sad1p-mEGFP and tdTomato-Mid1p. The top row is a composite image series of both Sad1p-mEGFP and mEGFP-Rng2p or mEGFP-Rng2pΔGRD (all shown in green) and tdTomato-Mid1p (shown in red). The middle row is an image series of the tdTomato-Mid1p signal only (shown in white) and the lower row is an image series of the Sad1p-CFP signal and mEGFP-Rng2p or mEGFP-Rng2pΔGRD signal (shown in white). (B) Times series of fluorescent micrographs recorded at 2 minute intervals at 32°C of *rng2-D5* cells expressing mEGFP-Rng2pΔRasGAP-C, Sad1p-RFP and mCherry-Cdc15p. The top row is a composite image series of mCherry-Cdc15p and Sad1p-RFP (both shown in red) and mEGFP-Rng2pΔRasGAP-C cells (shown in green). The middle row is an image series of the mCherry-Cdc15p signal and Sad1-RFP signal (shown in white) and the lower row is an image series of the mEGFP-Rng2pΔRasGAP-C signal only (shown in white). Time in min is shown in white with SPB separation defined as time zero.

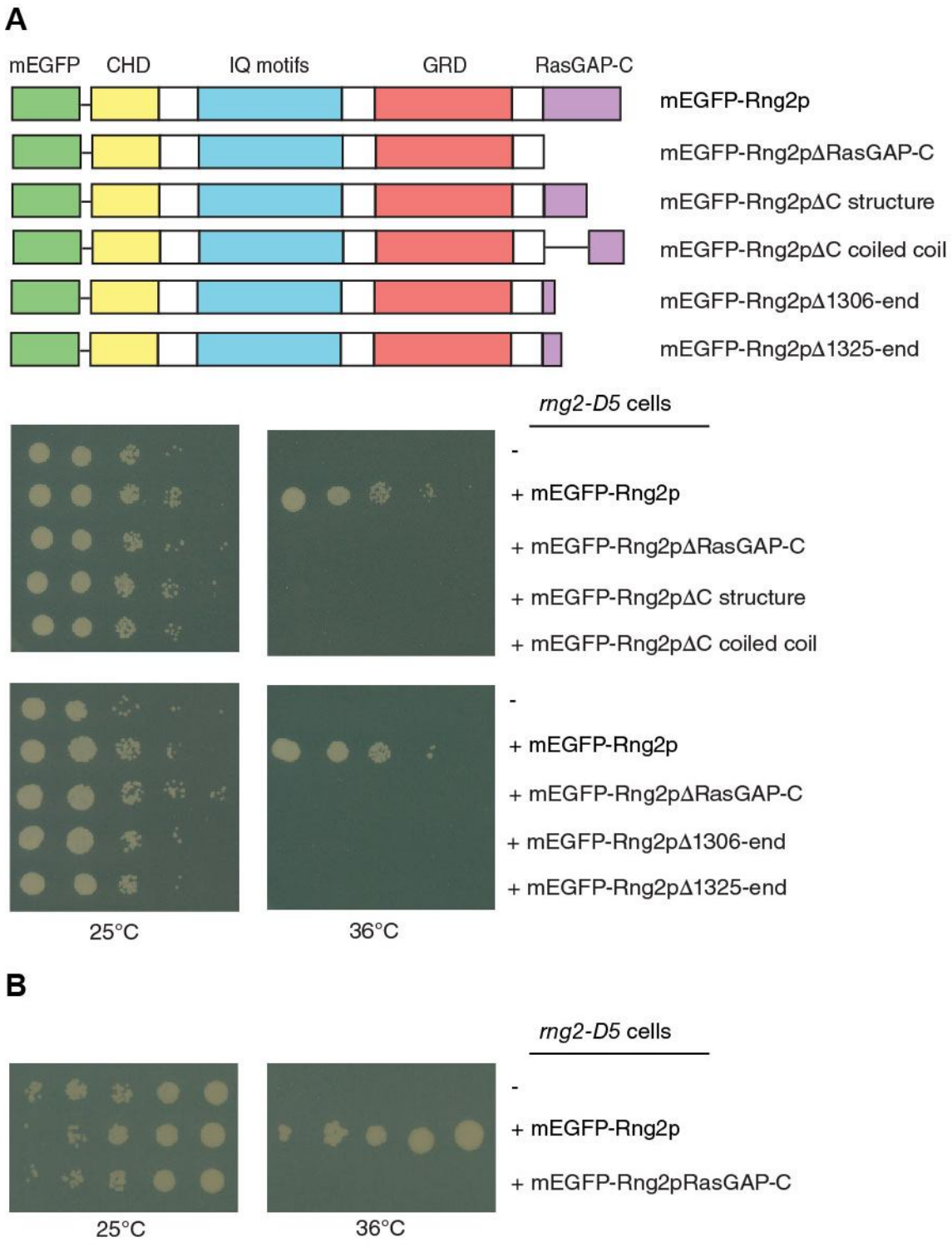

Figure S8. The entire C-terminal domain of Rng2p is required to rescue viability of *rng2-D5* cells. Schematic of domain architecture of mEGFP-Rng2p C-terminal deletion constructs inserted in the *leu1* locus. Complementation of *rng-D5* cells with mEGFP-Rng2p or mEGFP-

Rng2p C-terminal deletion constructs expressed from the *leu1* locus under the control of the *rng2* promoter. Photographs of agar plates with spots containing serial 1:10 dilutions of cells incubated 48 h at permissive (25°C) or restrictive (36°C) temperatures.

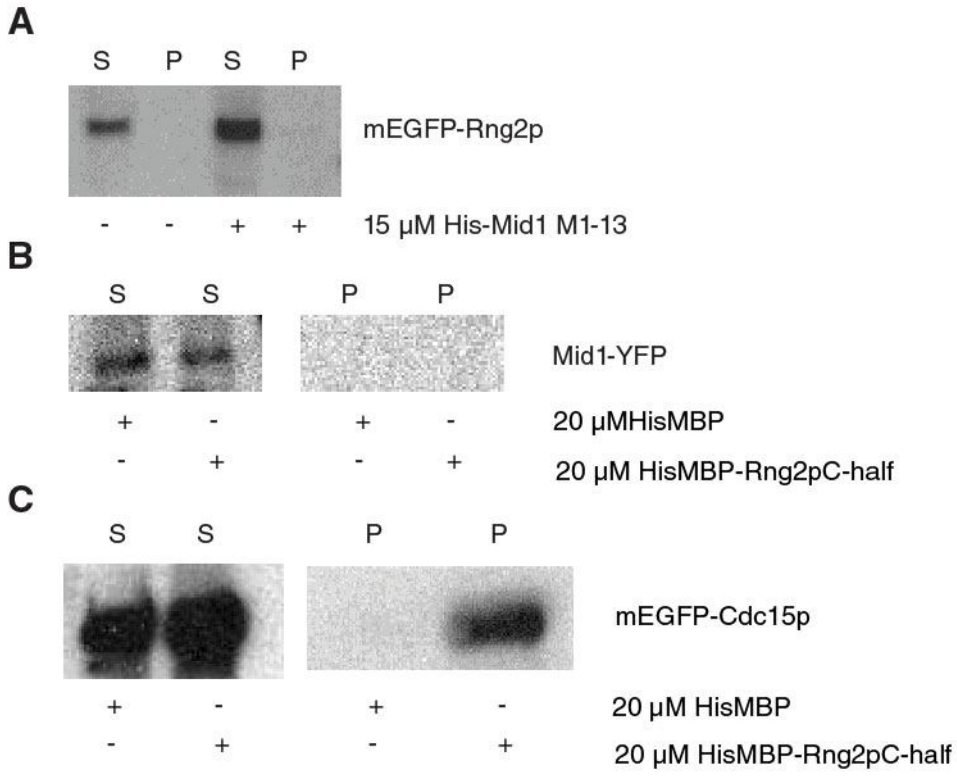

Figure S9. Western blots with antibodies to GFP from pulldown experiments to test for interactions of Mid1p with Rng2p**.** S is a sample from the supernatant. P is a sample from the pellet with the beads. **(**A) Ni-NTA beads with immobilized His-Mid1 M1-13 were incubated with cell lysates from mEGFP-Rng2p cells and pelleted. **(**B) Ni-NTA beads with immobilized His-MBP-Rng2p C-half were incubated with cell lysates from Mid1p-YFP cells. (C) Control experiment Ni-NTA beads with immobilized His-MBP-Rng2p C-half were incubated with cell lysates from mEGFP-Cdc15p cells.

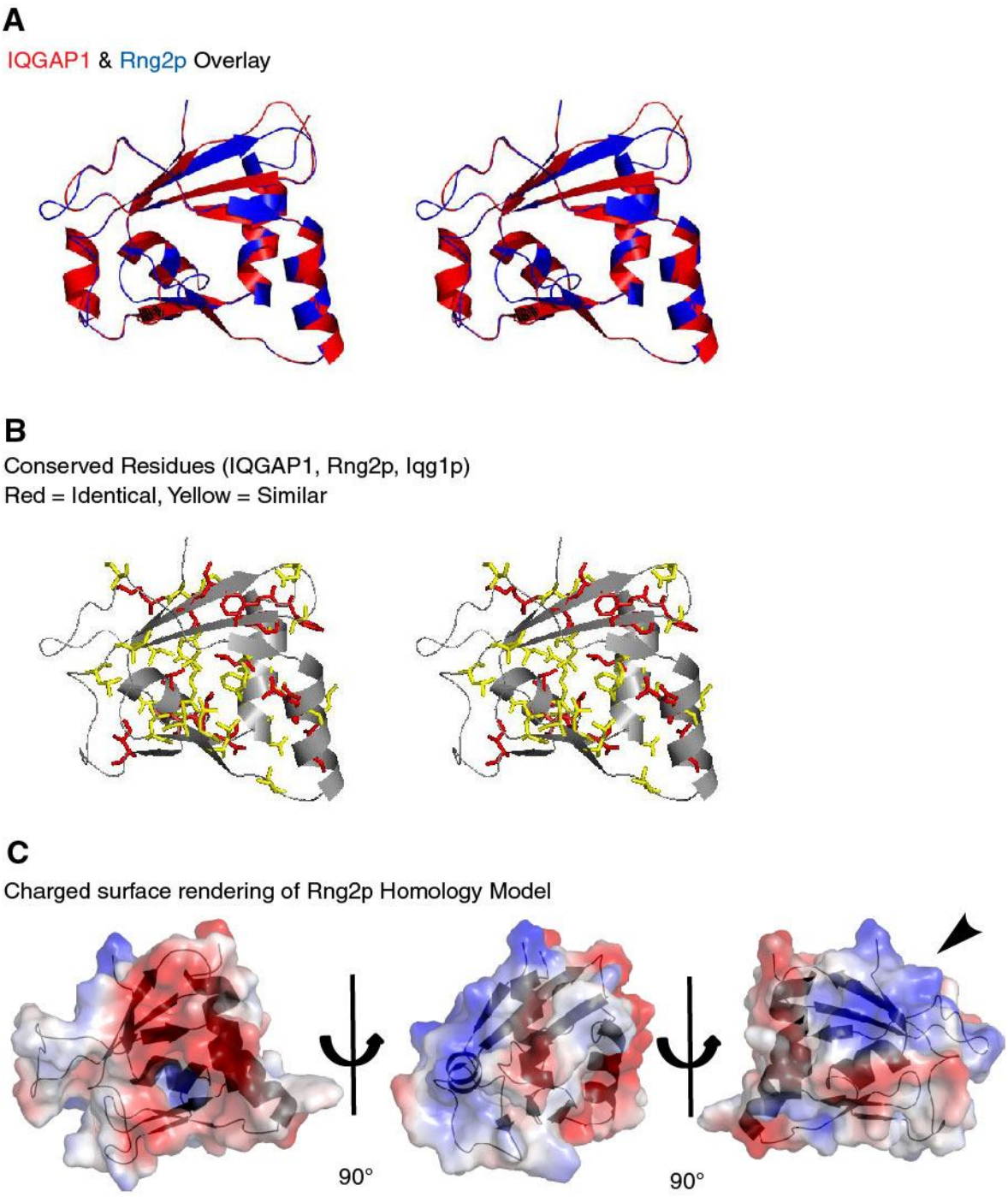

Figure S10. Homology models of Rng2p RasGAP-C based in an NMR structure of IQGAP1 (residues 1559-1657) (PDB 1X0H)**. (**A) Stereo ribbon diagram comparing in red the structure of IQGAP1 (1559-1657) with the homology model of Rng2p (1392-1489) in blue. (B) Stereo view of a ribbon diagram of the homology model of Rng2p (1392-1489) with stick figures of conserved residues in red (identical) or yellow (similar). (C) Three space-filling views with

internal ribbon diagrams of the homology model of Rng2p (1392-1489). Surface charges generated with the vacuum electrostatics function in Pymol are shown in red for negative regions and red for blue for positive regions. The black arrow head indicates the conserved area of positive charge.

Table S1. Summary of results

Genotype	Temp °C	Via-bility	Localization of Rng2 constructs	Time ring formed (min)	Maturation interval (min)	Time for constriction (min)
rng2^{+}	25 32 36	+ + +	Nodes and rings Nodes and rings	12.2 ± 2.6 7.7 ±1.4	23.1 ± 8.7 15.4 ± 3.3	28.6 ± 9.0 16.1 ± 2.4
mEGFP-rng2^{+}	25	+	Nodes and rings	13.4 ± 3.2[a]	22.8 ± 6.2	30.5 ± 3.8
mEGFP-81x-nmt-rng2 ($^{+}$ thiamine)	25	+/-	Nodes & rings in some cells, strands in others	24.6 ± 15.6[a]	17.1 ± 6.3	39.0 ± 9.3
rng2-D5	25 32 36	+ +/- -	Strands and rings Strands and rings	43.3 ± 24.2 40.0 ± 7.7	15.3 ± 8.2 5.5 ± 3.7	30.3 ±7.9 20.3 ±4.3
rng2-D5, mEGFP-rng2	32 36	+ +	Nodes and rings	7.1 ± 2.5		
rng2-D5, mEGFP-rng2ΔCHD	32 36	+ +	Nodes and rings	10.5 ± 2.5		
rng2-D5, mEGFP-rng2ΔIQ	32 36	+ +	Nodes and rings	15.2 ± 10.6		
rng2-D5, mEGFP-rng2ΔGRD	32 36	+ +	Strands and rings	20.9 ± 6.8		
rng2-D5, mEGFP-rng2ΔRasGAP-C	32 36	+/- -	Strands and rings	32.7 ± 4.6		
rng2Δ	25	-				
rng2Δ, mEGFP-rng2	25	+	Nodes and rings	8.8 ± 4.0	26.6 ± 2.3	25.3 ± 3.0
rng2Δ, mEGFP-rng2ΔCHD	25	+	Nodes and rings	9.9 ± 4.2	24.3 ±5.4	24.8 ± 2.3
rng2Δ, mEGFP-rng2ΔIQ	25	+	Nodes and rings	10.5 ± 3.9	56.3 ± 19.7	73.9 ± 11.1
rng2Δ, mEGFP-rng2ΔGRD	25	+	Strands and rings	24.9 ± 10.0	12.7 ± 4.4	25.7 ± 5.1
rng2Δ, mEGFP-rng2ΔRasGAP-C	25	-				

[a]: time begins with initial localization of Cdc15p to center of the cell rather than SPB separation.

References:

MacLean-Fletcher S, Pollard TD (1980) Identification of a factor in conventional muscle actin preparations which inhibits actin filament self-association. *Biochemical and biophysical research communications* **96:** 18-27

Saha S, Pollard TD (2012) Characterization of Structural and Functional Domains of the Anillin-related Protein Mid1p that Contribute to Cytokinesis in Fission Yeast. *Molecular biology of the cell*

Wang CH, Walsh M, Balasubramanian MK, Dokland T (2003) Expression, purification, crystallization and preliminary crystallographic analysis of the calponin-homology domain of Rng2. *Acta crystallographica Section D, Biological crystallography* **59:** 1809-1812